

DOI: 10.1002/elan.201900060

Electrochemical Sensor Based on Thioether Oligomer Poly(N-vinylpyrrolidone)-modified Gold Electrode for Bisphenol A Detection

Fairouz Aberkane,^{*,[a, b, c]} Abdoullatif Barakat,^[c] Abdelhamid Elaissari,^[b] Nadia Zine,^[c] Tahar Bendaikha,^[a] and Abdelhamid Errachid^[c]

Abstract: Presently, bisphenol A (BPA) has been added to the list of substances of very high concern as endocrine disruptors. According to the literature, exposure to bisphenol A even at low doses may result in adverse health effects. In this study, electrochemical sensor of Bisphenol A based on thioether DDT-Poly(N-vinylpyrrolidone) oligomer has been developed. The thioether oligomer, which is capable of recognizing BPA, was prepared and used for gold electrode modification. The characterization of the modified gold electrode and the synthesized thioether oligomer were carried out by cyclic voltammetry (CV), electrochemical impedance spectroscopy (EIS),

atomic force microscopy (AFM), Fourier-transform infrared spectroscopy (FTIR), proton nuclear magnetic resonance spectroscopy (¹H NMR) and Size exclusion chromatography (SEC). Obtained results indicate that the modified electrode shows good electrochemical activity, good sensitivity and reproducibility for BPA detection. It exhibited a good linear relationship ranging from 1 to 20 pg/mL, and the detection limit was found to be 1.9 pg/mL at S/N=3. Several interfering species such as hydroquinone, phenol and resorcinol were used and their behaviors on the modified gold electrode were investigated.

Keywords: Bisphenol A · Electrochemical sensor · Modified gold electrode · Thioether oligomer · Poly(N-vinylpyrrolidone).

1 Introduction

Bisphenol A (BPA) is classified as a Xenoestrogen compound; a type of xenohormone that imitates estrogen, which has estrogenic effects on a living organism. It can interfere with natural estrogenic substances produced by the endocrine system and disrupts hormonal levels [1,2]. BPA has been extensively studied since the 1930s in the search for synthetic estrogens as medications for hormonal disorder, but it has never been used, because of the discovery at the same time of diethylstilbestrol, which has properties deemed more interesting [3]. However, its use was only started in the 1950s by the plastics industry [4,5]. It has been used as a monomer in the manufacture of plastics such as polycarbonates and epoxy resins, as well as plasticizer, antioxidant or flame-retardant for other plastics. Plastic is widely used in our daily lives such as food packaging, water bottles, baby bottles, toys, lining canned food and beverages, medical materials and water pipes [6–8]. Unfortunately, it has been demonstrated that free BPA can leach from plastics under normal conditions of use. The rate of leaching accelerate as the temperature increases and in contact with acidic or basic substances [9]. Consequently, there is extensive human exposure to BPA, the current analytical techniques have detected BPA in over 95 % of human blood, serum, tissues, and urine [10]. According to the European Food Safety Authority (EFSA), the tolerable daily intake (TDI) for BPA is 4 µg/kg bw per day [11,12] and the new regulation introduces the specific migration limit (SML) of 0.05 mg

of BPA per kg of food. But, for the materials in contact with food for infants and young children, the new regulation prohibits the use of BPA as a precaution [13].

Food and drinks have been identified as the main source of BPA exposure in humans, due to its migration from the plastic containers to the food products. Research has shown that BPA is absorbed rapidly and efficiently into the gastrointestinal tract, converted to BPA-glucuronide and rapidly eliminated from the blood by urine. Nearly 100 % of exposed BPA is recoverable in urine within 24 hours [14]. Unfortunately, unconjugated BPA, its strength is as high as estradiol, which can act at very low doses and results in changes in certain cell functions at concentrations ranging from 1 pM to 1 nM [10,15,16]. Studies have reported that BPA can be measured in follicular fluid, amniotic fluid, placental tissue and um-

- [a] F. Aberkane, T. Bendaikha
University of Batna 1, Laboratory LCCE, Faculty of matter sciences, Department of chemistry, 05000 Batna, Algeria
E-mail: fairouz.aberkane@univ-batna.dz
- [b] F. Aberkane, A. Elaissari
Univ Lyon, University Claude Bernard Lyon 1, CNRS, LA-GEP-UMR 5007, F-69622 Lyon, France
- [c] F. Aberkane, A. Barakat, N. Zine, A. Errachid
Univ Lyon, University Claude Bernard Lyon 1, CNRS, ISA-UMR 5280, F-69622 Lyon, France

 Supporting information for this article is available on the WWW under <https://doi.org/10.1002/elan.201900060>

bilical cord blood [8,17]; there is considerable evidence that bioaccumulation of BPA can occur during pregnancy [10]. Some other studies suggest that the effects of BPA may be more pronounced in the fetus, infants and young children; they are less effective in removing substances from their systems [1]. The potential effects of BPA on the brain, behavior and prostate glands of fetuses, infants and young children have been studied [1]. Moreover, increased risks of cancer, obesity, diabetes, heart problems, reduce immune function and impaired reproduction in adults have been also investigated [2,18–20]. Therefore, it is very important to establish a reliable method for determination and monitoring BPA trace amounts and to evaluate the potential risks associated with cumulative low-dose exposures to BPA.

Currently, many analytical methods have been used for the determination of BPA such as high performance liquid chromatography (HPLC) [21,22], liquid chromatography-mass spectrometry [23,24], gas chromatography-mass spectrometry (GC-MS) [25,26], fluorescence analysis [27,28], colorimetric [29] and electrochemical methods [16,30–34]. However, electrochemical technics are most important due to their high sensitivity, simplicity, low cost, miniaturization, cheap instrument, fast and real time response compared to the other methods. The development of electrochemical sensors via a modifying electrode is a common strategy for the electrochemical detection of BPA. Therefore, various types of electrodes have been modified, for this purpose, with the use of enzymes [35], antibodies [36], chitosan [37], graphene [38,39], carbon nanotube [30], gold nanoparticles [27], quantum dots [40] and polymer [41,42].

In this research, thioether oligomer DDT-Poly(N-vinylpyrrolidone) has been prepared by a simple bulk radical polymerization in presence of a thermal initiator benzoyl peroxide (BPO) and transfer agent dodecanethiol (DDT). Resulting oligomer has been used for gold electrode modification for BPA sensing for the first time. The characterization of synthesized thioether oligomer DDT-Poly(N-vinylpyrrolidone) and the corresponding modified gold electrode were carried out by ^1H NMR, FTIR, size exclusion chromatography (SEC), cyclic voltammetry (CV), electrochemical impedance spectroscopy (EIS) and atomic force microscopy (AFM).

2 Experimental

2.1 Materials

All chemicals required for experiments were of analytical purity and used as received; N-vinyl pyrrolidone (NVP, +99%) was purchased from Aldrich. Hydroquinone (+99%), Resorcinol (99%) and Phosphate buffer saline were purchased from sigma. Phenol (>99.5%) was obtained from Riedel-DeHaën. Bisphenil A ($\geq 99\%$), Potassium hexacyanoferrate(II) trihydrate (>98.5%), Potassium hexacyanoferrate(III) (>99%), hexane ($\geq 99\%$) and chloroform ($\geq 99\%$) were purchased from Sigma-

Aldrich. 1-dodecanethiol (DDT, >97%) and Benzoyl peroxide (BPO, $\geq 99\%$) was obtained from Fluka. All the measurements were carried out at room temperature in a 0.01 M PBS buffer solution containing ions $[\text{Fe}(\text{CN})_6]^{3-/4-}$ at a concentration of 5 mM (pH = 7.4).

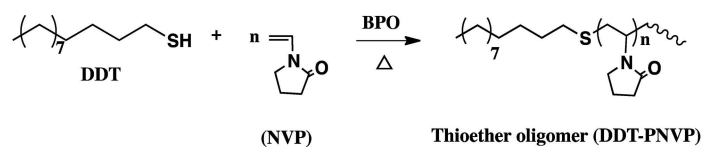
2.2 Methods

Electrochemical experiments were carried out with a VMP3 multichannel potentiostat (Biologic-EC-Lab, France) with a conventional three-electrode cell. A saturated calomel electrode (SCE) and a platinum electrode were used as reference electrode and auxiliary electrode, respectively. Gold working electrodes (WEs) (1 cm^2) based on 300 nm of gold coated onto silicon and silicon oxide substrate (Si/SiO_2) were used as transducer for the electrochemical sensor. WEs were fixed within the teflon electrochemical cell [43]. The surface of gold WEs exposed to the electrochemical measurements was 0.3 cm^2 .

Infrared spectra of monomer and synthesized thioether oligomer were recorded on FTIR spectrometer Nexus 470 (Thermoscientific France) in a total reflexing attenuated on crystal of diamond in monoreflexion (Smart-orbit, Thermo Scientific). The average weight and polydispersity of synthesized thioether oligomer was determined by using steric exclusion chromatography (SEC). The analyzes are carried out using an AGILENT 1200 Series isocratic pump equipped with an AGILENT 1200 Series, automatic switch and a set of columns. Detection is performed by an AGILENT 1260 Infinity Series Refractometer with debit of $1.0\text{ mL}\cdot\text{min}^{-1}$ in 30°C (columns). ^1H NMR spectrum was recorded in CDCl_3 on a Bruker AV400 MHz spectrometer at room temperature using the δ scale and tetramethylsilane (TMS) as an internal standard. Chemical shift was given in ppm relative to tetramethylsilane.

The hydrophilic character of the modified gold working electrodes (WEs) was investigated by contact angle measurements using 'Digidrop' from GBX (France). Here, $5\ \mu\text{L}$ of deionized water were dropped onto the modified electrode surface and the digital camera associated with the instrument captures the images. The contact angles were obtained from different areas of the WEs. The volume and the size of the water droplets were kept constant.

Atomic Force Microscopy (AFM) was performed in air under ambient conditions using a Nano observer (CSI Company, France). Measurements were made using silicon cantilever tip (ScienTec AppNano). The cantilever size L: $125\ \mu\text{m}$, W: $35\ \mu\text{m}$ and T: $4.5\ \mu\text{m}$. The tip radius: $< 10\ \text{nm}$, H: $14\text{--}16\ \mu\text{m}$ and with a frequency of $200\text{--}400\ \text{kHz}$ and spring constant of K: $25\text{--}75\ \text{N/m}$. The scanning images were performed at $669\ \text{mV}$ amplitude, $3.18\ \text{V}$ set point and Tip DC at $477\ \text{nV}$. Measurements were performed in taping mode with a speed of 0.25 lines per second and 511 resolutions.



Scheme 1. Radical polymerization reaction of NVP in the presence of DDT.

2.2.1 DDT-Poly(*N*-vinylpyrrolidone) Synthesis (DDT-PNVP)

The synthesis of thioether oligomer (DDT-PNVP) was carried out by the free-radical bulk polymerization as follow: 2 mL of *N*-vinyl pyrrolidone (NVP, 18,76 mmol) was heated at high temperature between 100 °C and 110 °C for 48 h in the presence of thermal initiator, benzoyl peroxide BPO (10 mg, 0.0413 mmol) and 0.96 mL of dodecanethiol (DDT, 4 mmol). The mixture was degassed for 30 min by using ultrasonic apparatus before heating in an oil bath. After cooling, viscous product, yellow to orange in color, was obtained. For removing unreacted monomer and oligomer with very low weight, the final product was dissolved in chloroform and re-precipitated in cold *n*-hexane several times. Oligomer thus obtained was dried, at ambient temperature then at 50 °C to a constant weight. The yield of thioether oligomer DDT-PNVP was 62.68 %.

2.2.2 Preparation of Modified Gold Electrode (GE/DDT-PNVP)

Gold substrate was washed twice with acetone in an ultrasonic bath for 15 min, followed by incubation in piranha solution ($\text{H}_2\text{SO}_4/\text{H}_2\text{O}_2:3\text{v}/1\text{v}$) for 5 min to remove the inorganic and organic impurities present on the surface. Then, the substrate was rinsed thoroughly with absolute ethanol and distilled water and finally dried with nitrogen. The cleaned gold substrate was incubated in the thioether oligomer solution (0.35 g/mL of DDT-PNVP) in chloroform for 48 hours at 4 °C. Prior to any electrochemical measurement, the gold substrate was rinsed with ethanol and distilled water several times to remove the unattached oligomer. The measurements were made in PBS buffer containing Ferro/Ferricyanide ions $\text{Fe}(\text{CN}_6)^{3-/4-}$ at a concentration of 5 mM (pH = 7.4).

3 Results and Discussion

3.1 Synthesis and Characterization of DDT-PNVP

DDT-PNVP was synthesized by the chain transfer radical polymerization method using NVP as a monomer and DDT as the chain-transfer agent (Scheme 1). The use of DDT is for the purpose of having a chain end containing sulfur. The polymerization reaction is initiated by a thermal initiator, benzoyl peroxide BPO at 100–110 °C for 48 h, in fact DDT also contributes to the initiation of the polymerization; sulfur has a great affinity to radicals and

can easily lose its thiol-hydrogen in radical form [44]. The molecular weight of the DDT-PNVP oligomer was determined using size exclusion chromatography (SEC). The average molecular weight (M_w) was found to be 1790 g/mol relative to polystyrene standards, with a polydispersity index (PDI) of 1.37. The calibration is carried out with polystyrene standards of increasing molecular weight (3600, 7200, 10050, 12900, 21720 g/mol). The molecular weight of *N*-vinylpyrrolidone is 111.14 g/mol corresponding to chain length approximately $PD = 16$ (polymerization degree). However, the low molecular weight of the polymer (<2000 g/mol) and the relatively narrow molecular weight distribution, are due to the radical polymerization technique used. ^1H NMR and FTIR spectroscopy were selected to validate the structure of the ligand DDT-PNVP oligomer (Figure. SI.1 and SI.2 in the supporting data).

FTIR spectrum of DDT-PNVP, provided in Figure SI.1 (in the supporting data), illustrate the absorption peaks at 2953.36 and 2892.91 cm^{-1} . These were associated with the asymmetric and symmetric stretching vibrations of aliphatic methylene ($-\text{CH}_2-$) and methyl ($-\text{CH}_3$) coming from oligomer and from DDT linked at its extremity. The band at 1662.98 cm^{-1} originates from the vibration of the carbonyl bond ($\text{C}=\text{O}$). The large band around 3440 cm^{-1} can be attributed to the O–H stretching vibrations; this is because the carbonyl groups can form hydrogen bonds with traces of water (moisture). The strong band at 1288.94 cm^{-1} was the stretching vibration of C–N bond. In the monomer (NVP) spectrum, the strong bands at 1629.24 cm^{-1} and 1705.05 cm^{-1} correspond to the absorptions of the double bond ($\text{C}=\text{C}$) and carbonyl bond respectively. The absorption peaks at 3109.03, 981.82 and 930.72 cm^{-1} were attributed to the bond ($=\text{C}-\text{H}$) of the double bond. The stretching vibration of C–N bond in the monomer appeared at 1285.8 cm^{-1} . On the spectrum of polymer, the band characteristics of vinyl group were disappeared, which clearly shows the disappearance of the monomer after the polymerization reaction and the purification step (Figure SI.1 in the supporting data).

The proton nuclear magnetic resonance (^1H NMR) spectra of the synthesized DDT-PNVP is presented in Figure SI.2 (in the supporting data). For protons of pyrrolidone group in NVP, the main chain methine (H_6) and methylene protons (H_5) are assigned around 3.6–4.01 ppm and 1.5–1.88 ppm, respectively. The side chain methylene protons are assigned in the range 3.0–3.42 ppm (H_7), 2.13–2.5 ppm (H_9), and 1.8–2.1 ppm (H_8) [45,46]. Signals located at 0.88, 1.25, 1.43 and 2.37 ppm are

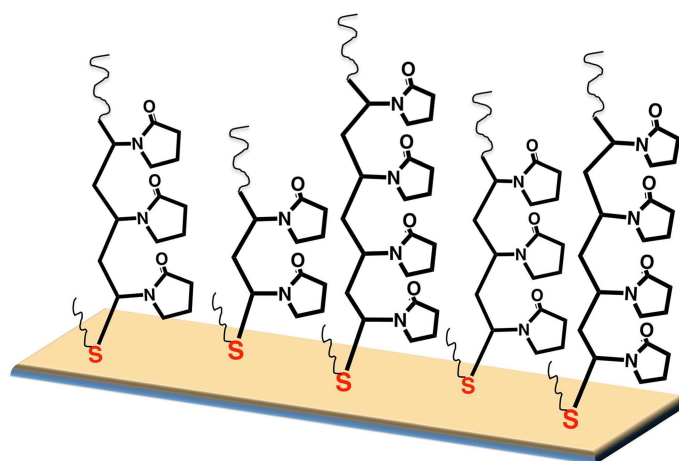


Fig. 1. Proposed morphology of gold electrode modified by thioether oligomer (GE/DDT-PNVP).

assigned to the aliphatic protons of the DDT fragment, linked to the chain end of the oligomer, H_1 , H_2 , H_3 and H_4 respectively [47].

3.2 Characterization of Modified Gold Electrode GE/DDT-PNVP

The GE/DDT-PNVP was prepared by a simple incubation of clean gold substrate in DDT-PNVP solution in chloroform. The presence of the DDT fragments at the end of the oligomer chain, which contain sulfur, helps the oligomer attach to the surface of gold, because sulfur atom is known by its affinity with gold. Thiol can form, according to the literature, monolayers on gold surfaces, with $\geq 85\%$ of their sulfur atoms forming bonds (Au–S) to the gold substrate [48]. Contrary to this, thioether retains its structure; there is many evidences confirming that thioether (dialkyl sulfides) molecules can be adsorbed on gold surface with double-chain conformation without C–S cleavage and most thioether molecules are held on the surface by “physisorption” [49,50]. Figure 1 shows a schematic illustration of the proposed morphology of GE/DDT-PNVP.

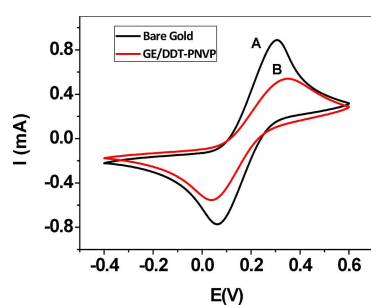


Fig. 2. Cyclic voltammograms of gold WEs (A) before and (B) after modification by DDT-PNVP. The measurements were made in PBS in the presence of $\text{Fe}(\text{CN})_6^{3-/4-}$, scan rate 100 mV/s.

The electrochemical properties of the modified gold WEs were determined by CV and by EIS. Figure 2 shows CV analysis of the gold WEs before and after chemical surface modification with DDT-PNVP. CV was recorded by varying the potential from -400 mV to $+600$ mV with a scan rate of 100 mV/s. For bare gold, a couple of redox peaks of $\text{Fe}(\text{CN})_6^{3-/4-}$ (supporting electrolyte) were observed with peak-to-peak separation (ΔI_p) of 1.66 mA and (ΔE_p) of 24.54 mV. When the substrate was covered with DDT-PNVP, a decrease of charge transfer was observed; a couple of redox peaks of $\text{Fe}(\text{CN})_6^{3-/4-}$ were obtained with peak-to-peak separation (ΔI_p) of 1.09 mA and (ΔE_p) of 31.26 mV. The decrease in current indicates that DDT-PNVP could effectively decrease the electron transfer rate between the gold electrode surface and $\text{Fe}(\text{CN})_6^{3-/4-}$ solution which could be attributed to the bad conductivity of DDT-PNVP.

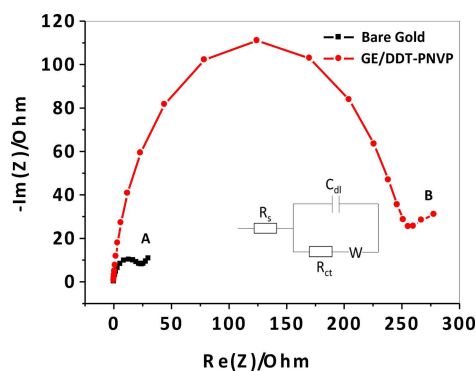


Fig. 3. Nyquist plots of bare gold WEs (A) and DDT-PNVP modified gold WEs (B). The EIS were recorded in the presence of $\text{Fe}(\text{CN})_6^{3-/4-}$ at a frequency range between 1 Hz and 200 kHz, at a potential of 0.2 V. The impedance behavior of the electrolyte can be fitted to a Randles model; that includes the solution resistance (R_s), charge transfer resistance (R_{ct}), constant phase element (C_{dl}) and Warburg impedance element (W).

Nyquist plots presented in Figure 3 clearly demonstrate the impedance difference between unmodified and DDT-PNVP modified gold WEs. The first Nyquist plot semi-circle corresponds to bare gold with low transfer charge resistance (R_{ct}) at the interface electrode/electrolyte. After the modification with DDT-PNVP, the diameter of the Nyquist plot semi-circle was much larger with high impedance. This increased impedance (increase of R_{ct}) was induced by the formation of thioether oligomer layer, on the gold WEs, and implying good blocking behavior and complete control of charge transfer for the transfer process. The Faradaic impedance measurements are in good agreement with CV measurements. The recovery rate was calculated by using the equation (1) and found to be $\theta=67.66\%$. The interaction type of the thioether with gold surface can explain the low value of the recovery rate; thioether adsorb on the surface of gold with a double-chain conformation and this structure is more congested and leads to a low density [50].

$$\theta = 1 - \frac{R_{ct_0}}{R_{ct}} \quad (1)$$

Where, R_{ct_0} is the charge transfer resistance at bare gold and R_{ct} is the charge transfer resistance at the GE/DDT-PNVP under the same condition.

The chemical surface modification was also confirmed by the wettability study using water contact angle measurements. A camera recorded the image of the water droplet deposited on the gold electrode surface and the contact angle was calculated from the droplet shape by an image-analysis system. The contact angle value for the bare gold was found to be 67.19° ; while after treatment with the piranha solution a decrease in the contact angle value was observed (33.49°). After the modification with DDT-PNVP, the contact angle of the modified gold substrate revealed a slightly increase from 33.49° to 45.88° (Figure SI.3 in the supporting data), which confirms that the surface has been modified and the sensing film was deposited on the gold WEs surface.

Electrochemical active surface area of GE/DDT-PNVP was determined by Chronoamperometry. In this method, the potential of the working electrode is stepped and the resulting current from faradaic processes occurring at the electrode is monitored as a function of time. In chronoamperometric studies, the current for the electrochemical reaction of ferrocyanide, that diffuse to a electrode surface, is described by the Cottrell equation (Eq.2) [51], which defines the current-time dependence for linear diffusion control.

$$I_{(t)} = nFAC\sqrt{\frac{D}{\pi t}} \quad (2)$$

$$\text{Slope} = nFAC\sqrt{\frac{D}{\pi}} \quad (3)$$

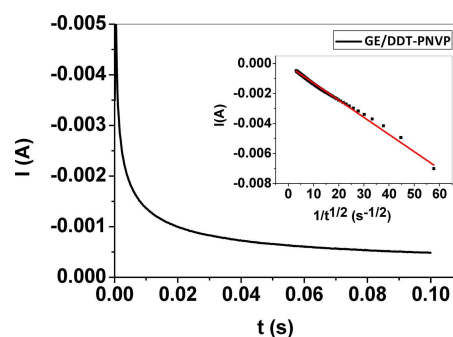


Fig. 4. Plot of I - t curve of GE/DDT-PNVP in PBS containing 5 mM $\text{Fe}(\text{CN})_6^{3-/4-}$ at a potential of 0.2 V; and the plot of I - $t^{-1/2}$ curve derived from the data of chronoamperometry for the same sample as inset ($I_{(t)} = 10^{-4} (-1.517 - 1.1454 t^{-1/2})$, $R^2 = 0.99$).

Where, n is the number of electrons involved, A is the electrochemical active area, F is the Faraday constant ($96500 \text{ C}\cdot\text{mol}^{-1}$), D is the diffusion coefficient ($7.6 \cdot 10^{-6} \text{ cm}^2\cdot\text{s}^{-1}$) and C is the concentration of $\text{Fe}(\text{CN})_6^{3-/4-}$ (5 mM). Figure 4 depicts typical chronoamperometric response, I vs t plot at a potential of 0.2 V and the resulting I vs $t^{-1/2}$ representation. The chronoamperogram I vs $t^{-1/2}$ plot was found to be straight line ($R^2 = 0.99$). From the slope (Eq.3) the electrochemical active area of the GE/DDT-PNVP electrode obtained was 0.15 cm^2 .

AFM was also used to characterize the topography modification of gold WEs before (A) and after chemical surface modification (B). Figure 5 shows gold surface topography and the surface morphology as well as the film thickness of DDT-PNVP deposited on gold WE (B). At the micrometric scale, the oligomer layer is in the form of relatively dense and homogeneous globules. The roughness parameter was calculated in order to permit the comparison of the layer density after modification. The bare gold has a roughness factor of 0.43 nm, after modification the oligomer layer has a roughness factor of

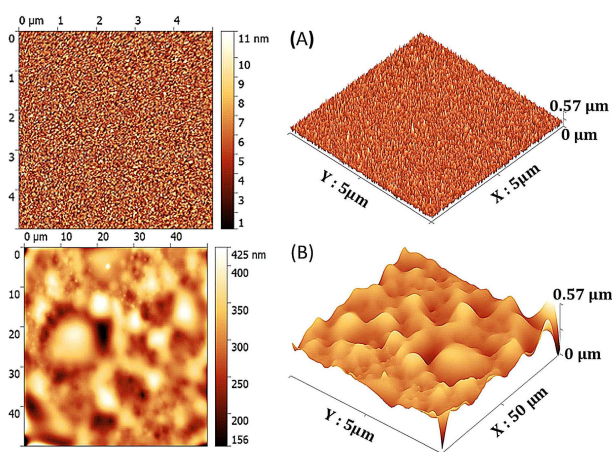


Fig. 5. AFM images of gold WEs: (A) bare gold and (B) GE/DDT-PNVP.

3.7 nm. This increase of roughness factor confirms the surface modification of the gold substrate.

3.3 Electrochemical Behavior of Bisphenol A on DDT-PNVP Modified-gold Electrode

The prepared GE/DDT-PNVP was immersed during 30 min into solution containing BPA with different concentrations ranging from 1 pg/mL to 20 pg/mL. After each incubation, the electrochemical sensor was washed with absolute ethanol and water. EIS measurements were carried out, after each incubation, in a 0.01 M PBS buffer solution containing $\text{Fe}(\text{CN})_6^{3-/4-}$ at a concentration of 5 mM (pH=7.4) within the frequency range from 1 Hz to 200 KHz and at a potential of 0.2 V. Figure 6, shows a distinct EIS response (Nyquist diagram (A) and the corresponding Bode plots (B)) of the GE/DDT-PNVP for different concentrations of BPA. The first Nyquist plot semi-circle corresponds to blank GE/DDT-PNVP. After incubation of the electrochemical sensor in BPA for 30 min, the second Nyquist plot semi-circle has shifted and decreased from the first highlighting thus the adsorption of BPA onto the sensitive membrane. The radius of the semicircles, in the Nyquist plots, decrease linearly with increasing BPA concentration. The efficient trapping of BPA molecules within thioether oligomer caused the increase in electrochemical current. In the work of Dahlia C. Apodaca et al, they also found, that the total impedance, obtained during the rebinding of the different concentrations of BPA on the imprinted film, decreases with an increase in BPA concentration [52]. The equivalent electrical circuit shown in Figure 5 modeled resulting impedance spectra, obtained in the

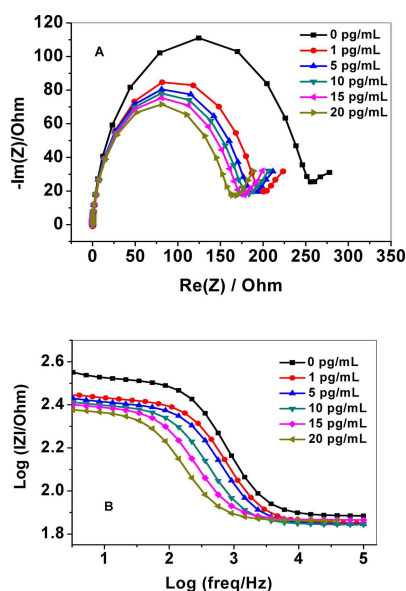


Fig. 6. EIS analysis in PBS containing 5 mM $\text{Fe}(\text{CN})_6^{3-/4-}$, obtained from the increasing concentration of BPA from 1 to 20 pg/mL at a potential of 0.2 V: (A) Nyquist plots and (B) Bode plots of GE/DDT-PNVP electrode. Measurements was.

presence of different concentrations of BPA. The binding mechanism between BPA and the oligomer may be explained by the formation of hydrogen bonds; hydroxyl groups in the BPA molecules (on both ends) and nitrogen or oxygen presented along the oligomer chains favored the formation of these interactions (hydrogen bonds). This would imply, that the binding opens up channels in the adlayer such that $\text{Fe}(\text{CN})_6^{3-/4-}$ can reach the surface and undergo electronic transfer. This phenomenon increase with increasing BPA concentrations. Chemical adsorption energy of BPA molecules binding to the oligomer layer can be calculated by using Langmuir equation [53,54], and it was found to be $\Delta G^\circ = -65.19$ KJ/mol with a high adsorption constant $0.2712 \cdot 10^9$ L/g (SII in the supporting data).

To evaluate the detection limit (LOD), sensitivity and the linear response range, a calibration curve was formed (Figure 7). In this calibration curve, the analytical signal ($\Delta R/R = (R_{ct} - R_{ct_0})/R_{ct_0}$) is plotted versus the concentration of BPA. The linear relationship ($R^2 = 0.9885$) between the $\Delta R/R$ and the concentration of BPA is according to the equation: $\Delta R/R = -0.01017[\text{BPA}] - 0.29469$. All the measurements were performed with $n = 3$ replicates. The detection limit was calculated from $\text{LOD} = 3\text{SD}/b$, where (SD) is the standard deviation of intercept of the linear calibration curve for three independent curves and (b) is the slope of the calibration curve [55]. The LOD was found to be 1.9 pg/mL at $S/N = 3$ (equivalent to 8.32 pM), and the sensitivity ($0.01 \text{ pg}^{-1}/\text{mL}^{-1}$) is the slope of the calibration curve. In addition, it was obtained a calibration curve with a linear range from 1 to 20 pg/mL (equivalent to 4.38–87.71 pM). The characteristics of relevant and previous modified electrodes for BPA detection in terms of the concentration range and detection limit are given in Table 1. Furthermore, The reproducibility of the modified electrode GE/DDT-PNVP was evaluated by the measurement of the response to 10 pg/mL of BPA in 0.01M PBS containing 5 mM Ferro/Ferricyanide ions by impedance spectroscopy. We prepared three different BPA sensors with the same modification. The relative standard deviation was calculated and found to be 6.72 %, indicating that the proposed sensor has good reproducibility.

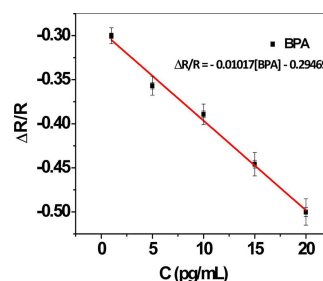


Fig. 7. Calibration plot of the BPA modified gold electrode sensor.

Table 1. A comparison of the analytical characteristics of the modified electrode developed in this work with relevant modified electrodes for BPA detection based in the literature.

Electrode	Method	Linear range	LOD	Ref
MIP MWCNTs-GNPs/GE	Amperometric	$1.13 \cdot 10^{-7}$ – $8.21 \cdot 10^{-3}$ M	3.6 nM	[30]
MIP PPy-TiO ₂ NTs	PEC	4.5–108 nM	2 nM	[31]
GO-MNPs/CGE	CV	$6.10 \cdot 10^{-8}$ – $1.1 \cdot 10^{-5}$ M	$1.7 \cdot 10^{-8}$ M	[38]
AuNPs/PVP/PGE	SWAdSV	0.03–1.1 μ M	0.02 μ M	[42]
GO-Cu ₂ O/GCE	CV	0.1–80 μ M	$5.3 \cdot 10^{-8}$ M	[56]
GNPs-AuNPs/GCE	DPV	$5.10 \cdot 10^{-3}$ –100 μ M	0.027 nM	[57]
MCH/Aptamers/Au-NPs/BDD	Impedimetric	$1.0 \cdot 10^{-14}$ – $1.0 \cdot 10^{-9}$ M	$7.2 \cdot 10^{-15}$ M	[58]
DDT-PNVP/GE	Impedimetric	4.38 pM–87.6 pM	8.32 pM	This work

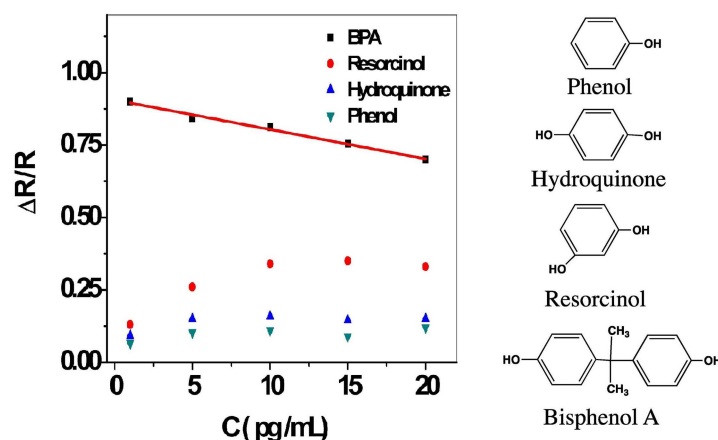


Fig. 8. Calibration plots of GE/DDT-PNVP in BPA, Hydroquinone, Phenol and Resorcinol sensing.

In this work, selectivity of the developed chemical sensor has also been studied for BPA over other interfering species, which have the same functional group as BPA (hydroxyl function). Here, Phenol, hydroquinone and resorcinol, which are used usually in plastic manufacture as a monomer, stabilizer or inhibitor, were used to check selectivity of the present sensor. As shown in Figure 8, the calibration curves, obtained after incubation of GE/DDT-PNVP in different concentrations of interfering products between 1 and 20 pg/mL, are not linear. This indicates that the GE/DDT-PNVP has no sensitivity for both phenol, hydroquinone and resorcinol products.

4 Conclusion

In the present work, an electrochemical sensor of bisphenol A has been developed by a very simple method. A thioether DDT-poly(N-vinylpyrrolidone) oligomer has been synthesized and used to modify the surface of a gold electrode. The thioether oligomer represents the sensitive layer in the chemical sensor. Synthesis of oligomer has been carried out by radical polymerization in the presence of dodecanethiol as a transfer agent, leading to formation of polymer chains with an end chain containing sulfur. Sulfur atom has a remarkable affinity for noble metals, which helps the oligomer chains to be attached on gold surface and leading to stable layer formation. Achieved

results demonstrate that the oligomer-based sensor has good reproducibility and appreciable sensitivity ($0.01 \text{ pg}^{-1}\text{mL}^{-1}$) for BPA and exhibits excellent performance for BPA determination with a good linearity relationship for concentration ranging from 1 pg/mL to 20 pg/mL (equivalent to 4,38 pM–87.71 pM), with detection limit of 1.9 pg/mL (8.32 pM) at $S/N=3$. Several interfering compounds, such as phenolic (phenol, hydroquinone and resorcinol) were used and their behaviors on the modified gold electrode were investigated. The obtained results demonstrate that the elaborated GE/DDT-PNVP electrode was found to be more sensitive to BPA than Phenol, resorcinol and hydroquinone.

Acknowledgement

We acknowledge the funding through the European Union's Horizon2020 research and innovation program entitled KardiasTool under grant agreement No 768686.

References

- [1] J. Stragierowicz, *IJOMEH*. **2015**, 28(2), 209–241.
- [2] J. Michałowicz, *Environ. Toxicol. Pharmacol.* **2014**, 37, 738–758.
- [3] E. Ribeiro, C. Ladeira, S. Viegas, *Toxicol* **2017**, 5, 22.

- [4] S. Eladak, T. Grisin, D. Moison, M. J. Guerin, T. N'Tumba-Byn, S. Pozzi-Gaudin, A. Benachi, G. Livera, V. Rouiller-Fabre, R. Habert, *Fertil. Steril.* **2015**, *103*, 11–21.
- [5] F. S. vom Saal, *Reprod. Toxicol.* **2007**, *24*, 131–138.
- [6] J. E. Biles, T. P. McNeal, T. H. Begley, H. C. Hollifield, *J. Agric. Food Chem.* **1997**, *45*, 3541–3544.
- [7] N. N. Maserejian, R. Hauser, M. Tavares, F. L. Trachtenberg, P. Shrader, S. McKinlay, *J. Dent. Res.* **2012**, *91* (11), 1019–1025.
- [8] L. N. Vandenberg, R. Hauser, M. Marcus, N. Olea, W. V. Welshons, *Reprod. Toxicol.* **2007**, *24*, 139–177.
- [9] P. Mercea, *J. Appl. Polym. Sci.* **2009**, *112*, 579–593.
- [10] W. V. Welshons, S. C. Nagel, F. S. Saal, *Endocrinology.* **2006**, *147*(6), s56–s69.
- [11] U. Gundert-remy, J. Bodin, C. Bosetti, R. Fitzgerald, A. Hanberg, C. Hooijmans, A. A. Rooney, C. Rousselle, H. Van Loveren, F. Barizzzone, C. Croera, C. Putzu, A. F. Castoldi, *EFSA Support. Publ.* **2017**, *14* (12), 1354E.
- [12] P. Aids, *EFSA Journal.* **2015**, *13*(1), 3978.
- [13] Commission Regulation (Eu) 2018/213. *Official Journal of the European Union.* **2018**, 6–12.
- [14] T. Tsukiokai, J. Terasawai, S. Sato, Y. Hatayamai, T. Makino, H. Nakazawa, *J. Environ. Chem. Eng.* **2004**, *14*(1), 57–63.
- [15] Y. B. Wetherill, B. T. Akingbemi, J. Kanno, J. A. Mclachlan, A. Nadal, C. Sonnenschein, C. S. Watson, R. T. Zoeller, S. M. Belcher, *Reprod. Toxicol.* **2007**, *24*, 178–198.
- [16] U. Karabiberog, *Electroanalysis.* **2019**, *31*(1), 91–102.
- [17] Y. Ikezaki, O. Tsutsumi, Y. Takai, Y. Kamei, Y. Taketani, *Hum. Reprod.* **2002**, *17*(11), 2839–2841
- [18] S. Nomiri, R. Hoshyar, C. Ambrosino, C. R. Tyler, B. Mansouri, C. R. Tyler, *Environ. Sci. Pollut. Res. Int.* **2019**, *26*, 8459–8467.
- [19] Y. Zhou, Z. Wang, M. Xia, S. Zhuang, X. Gong, J. Pan, C. Li, R. Fan, Q. Pang, S. Lu, *Environ. Pollut.* **2017**, *229*, 40–48.
- [20] S. Santangeli, F. Maradonna, I. Olivotto, C. Carla, G. Gioacchini, O. Carnevali, *Gen. Comp. Endocrinol.* **2016**, *245*, 122–126.
- [21] Y. Sun, M. Irie, N. Kishikawa, M. Wada, N. Kuroda, K. Nakashima, *Biomed. Chromatogr.* **2004**, *18*, 501–507.
- [22] M. Rezaee, E. Enginee, S. Shariati, R. Branch, M. Sciences, *J. Chromatogr. A* **2009**, *1216*(9), 27, 1511–1514.
- [23] N. C. Maragou, E. N. Lampi, N. S. Thomaidis, M. A. Koupparis, *J. Chromatogr. A* **2006**, *1129*, 165–173.
- [24] C. Liao, K. Kannan, *Environ. Sci. Technol.* **2012**, *46*(9), 5003–5009.
- [25] M. del Olmo, A. González-Casado, N. A. Navas, J. L. Vilchez, *Anal. Chim. Acta* **1997**, *346*(1), 87–92.
- [26] G. Gatidou, N. S. Thomaidis, A. S. Stasinakis, T. D. Lekkas, *J. Chromatogr. A* **2007**, *1138*, 32–41.
- [27] X. Wu, Z. Zhang, J. Li, H. You, Y. Li, L. Chen, *Sens. Actuators B* **2015**, *211*, 507–514.
- [28] J. Zhang, S. Zhao, K. Zhang, J. Zhou, *Chemosphere.* **2014**, *95*, 105–110.
- [29] J. Xu, Y. Li, J. Bie, W. Jiang, J. Guo, *Microchim. Acta* **2015**, *182*, 2131–2138.
- [30] J. Huang, X. Zhang, Q. Lin, X. He, X. Xing, H. Huai, W. Lian, H. Zhu, *Food Control.* **2011**, *22*, 786–791.
- [31] B. Lu, M. Liu, H. Shi, X. Huang, G. Zhao, *Electroanalysis.* **2013**, *25*, 771–779.
- [32] J. Han, F. Li, L. Jiang, K. Li, Y. Dong, Y. Li, *Anal. Methods.* **2015**, *7*, 8220–8226.
- [33] H. Ali, S. Mukhopadhyay, N. R. Jana, *New J. Chem.* **2019**, *43*, 1536–1543
- [34] A. Thamilselvan, V. Rajagopal, V. Suryanarayanan, *J. Alloys Compd.* **2019**, *786*, 698–706.
- [35] D. G. Mita, A. Attanasio, F. Arduini, N. Diano, V. Grano, U. Bencivenga, S. Rossi, A. Amine, D. Moscone, *Biosens. Bioelectron.* **2007**, *23*, 60–65.
- [36] K. Nishi, M. Takai, K. Morimune, H. Ohkawa, *Biosci. Biotechnol. Biochem.* **2003**, *67*, 1358–1367.
- [37] C. Yu, L. Gou, X. Zhou, N. Bao, H. Gu, *Electrochim. Acta* **2011**, *56*, 9056–9063.
- [38] Y. Zhang, Y. Cheng, Y. Zhou, B. Li, W. Gu, X. Shi, Y. Xian, *Talanta.* **2013**, *107*, 211–218.
- [39] S. Güneş, O. Güneş, *Electroanalysis.* **2017**, *29*, 2579–2590.
- [40] H. Yin, Y. Zhou, S. Ai, Q. Chen, X. Zhu, X. Liu, L. Zhu, *J. Hazard. Mater.* **2010**, *174*, 236–243.
- [41] J. Wang, Y. Su, B. Wu, S. Cheng, *Talanta.* **2016**, *147*, 103–110.
- [42] Y. T. Yaman, S. Abaci, *Sensors* **2016**, *16*, 756.
- [43] M. Bougrini, A. Baraket, T. Jamshaid, A. El Aissari, J. Bausells, M. Zabala, N. El Bari, B. Bouchikhi, N. J. Renault, A. Errachid, N. Zine, *Sens. Actuators B* **2016**, *234*, 446–452.
- [44] X. Huang, B. Li, H. Zhang, I. Hussain, L. Liang, B. Tan, *Nanoscale.* **2016**, *3*, 1600–1607.
- [45] J. Murakami, I. Kaneko, N. Kimata, M. Mineshima, T. Akiba, *Ren. Replace. Ther.* **2016**, *2*, 36.
- [46] W. Herrera, J. Cauich, *J. Therm. Anal. Calorim.* **2011**, *104*, 737–742.
- [47] J. Jayabharathi, G. A. Sundari, V. Thanikachalam, P. Jeeva, S. Panimozhi, *RSC Adv.* **2017**, *7*, 38923–38934.
- [48] H. J. Lee, A. C. Jamison, T. R. Lee, *Langmuir* **2015**, *31*, 2136–2146.
- [49] M. W. J. Beulen, B.-H. Huisman, P. A. van der Heijden, F. C. J. M. van Veggel, M. G. Simons, E. M. E. F. Biemond, P. J. de Lange, D. N. Reinhoudt, *Langmuir* **1996**, *12*, 6170–6172.
- [50] H. Takiguchi, K. Sato, T. Ishida, K. Abe, K. Yase, K. Tamada, *Langmuir* **2000**, *16*, 1703–1710.
- [51] A. J. Bard, L. R. Faulkner, *Electrochemical Methods: Fundamentals and Applications*, 2nd ed, John Wiley & Sons, Inc. **2001**, pp. 161–164.
- [52] D. C. Apodaca, R. B. Pernites, R. Ponnappati, F. R. Del Mundo, R. C. Advincula, *Macromolecules.* **2011**, *44*, 6669–6682.
- [53] B. M. Mistry, N. S. Patel, S. Sahoo, S. Jauhari, *Bull. Mater. Sci.* **2012**, *35*, 459–469.
- [54] Z. V. P. Murthy, K. Vijayaragavan, *Green Chem. Lett. Rev.* **2014**, *7*(3), 209–219.
- [55] A. Shrivastava, V. B. Gupta, *Chron. Young Sci.* **2011**, *2*(1), 21–25.
- [56] R. Shi, J. Liang, Z. Zhao, A. Liu, Y. Tian, *Talanta.* **2017**, *169*, 37–43.
- [57] J. Zou, G. Zhao, J. Teng, Q. Liu, X. Jiang, F. Jiao, J. Yu, *Microchem. J.* **2019**, *145*, 693–702.
- [58] Y. Ma, J. Liu, H. Li, *Biosens. Bioelectron.* **2017**, *92*, 21–25.

Received: January 25, 2019

Accepted: June 3, 2019

Published online on July 1, 2019